[Letter] Size selection of liquid-exfoliated 2D nanosheets

Article (Accepted Version)

2D Materials

Size selection of liquid-exfoliated 2D nanosheets

To cite this article before publication: Sean Paul Ogilvie *et al* 2019 *2D Mater.* in press https://doi.org/10.1088/2053-1583/ab0dc3

Size selection of liquid-exfoliated 2D nanosheets

Sean P. Ogilvie[a*], Matthew J. Large[a], Marcus A. O'Mara[a], Peter J. Lynch[a], Cheuk Long Lee[a], Alice A. K. King[a], Claudia Backes[b], Alan B. Dalton[a*]

[a] Department of Physics and Astronomy, University of Sussex, Brighton, BN1 9RH, United Kingdom

[b] Chair of Applied Physical Chemistry, Ruprecht-Karls University Heidelberg, 69120 Heidelberg, Germany

Keywords: two-dimensional materials, liquid exfoliation, centrifugation, size selection

Abstract

Here we present a size selection model for liquid-exfoliated two-dimensional nanosheets. The ability to consistently select exfoliated nanosheets with desired properties is important for development of applications in all areas. The model presented facilitates determination of centrifugation parameters for production of dispersions with controlled size and thickness for different materials, solvents and exfoliation processes. Importantly, after accounting for the influence of viscosity on exfoliation, comparisons of different solvents are shown to be well described by the surface tension and Hansen parameter matching. This suggests that previous analyses may have overestimated the relative performance of more viscous solvents. This understanding can be extended to develop a model based on the force balance of nanosheets falling under viscous drag during centrifugation. By considering the microscopic aspect ratio relationships, this model can be both calibrated for size selection of nanosheets and compare the exfoliation processes themselves.

Introduction

Liquid phase exfoliation has been demonstrated to be a versatile, scalable and cost-effective technique for the production of few-layer two-dimensional (2D) nanosheets for a wide range of layered materials and applications[1–6]. Although surfactants in aqueous solution have been shown to yield high-quality dispersions of few-layer nanosheets at reasonable concentrations owing to stabilisation by the amphiphilic surfactant molecules, their presence can often be undesirable for some applications[7]. Moreover, in certain cases it would be preferable to produce high-quality dispersions in organic solvents[8–10]. As a result, there has been extensive work to identify 'good' solvents based on the chemical physics of their interactions with the nanosheets through surface tension and Hansen solubility parameters [1,11,12].

The most commonly used and well-studied method for liquid phase exfoliation of 2D materials is probe ultrasonication, where high frequency ultrasound is applied to a high mass concentration dispersion of bulk layered material in liquid [1,12]. The sonication process both exfoliates and cuts the layered materials to yield a dispersion of particles with a wide distribution of size and thickness; from unexfoliated crystallites to monolayer nanosheets. After sonication, dispersions are typically subjected to centrifugation-based size selection where increased relative centrifugal forces result in accelerated and preferential sedimentation of the larger particles, leaving the few-layer nanosheets dispersed in the supernatant.

In addition to the considerations of surface tension and Hansen parameters, the physical properties of the solvents typically employed will influence the exfoliation, size selection and stability of the liquid-exfoliated nanosheets due to their effect on buoyancy, viscous drag, etc. An understanding of the influence of various processing parameters (sonication time and power, relative centrifugal force, etc.) on concentration, size and thickness of the exfoliated nanosheets has been developed through an iterative approach and is well described by scaling laws to maximise yield and the degree of exfoliation. However, there is little physical interpretation of this understanding (i.e. of the exponents and pre-factors of these scaling laws) to generalise the applicability to different materials and solvents. Here we study the influence of these factors to develop exfoliation processes, which apply to different 2D

materials and solvents. In particular, our results point to the role of viscosity in determining exfoliation yield during probe sonication and size selection during centrifugation. Accordingly, we develop a model based on the force balance of nanosheets falling under viscous drag during centrifugation that well describes size selection. This will allow others in the field to produce dispersions with desired properties for their chosen applications.

Results and discussion

During sonication, a probe oscillates at a fixed ultrasonic frequency and the amplitude (as a percentage of the maximum tip displacement) can be controlled as an experimental parameter. Although this complicated process depends on many factors such as vessel size and shape[13], the absolute power delivered by the probe is determined by the resistance to oscillation and therefore is primarily related to the viscosity of the liquid being sonicated. As such, the power output and therefore total energy delivered during ultrasonication-based exfoliation cannot be independently controlled, preventing a direct comparison of the exfoliation processes in solvents with different viscosities.

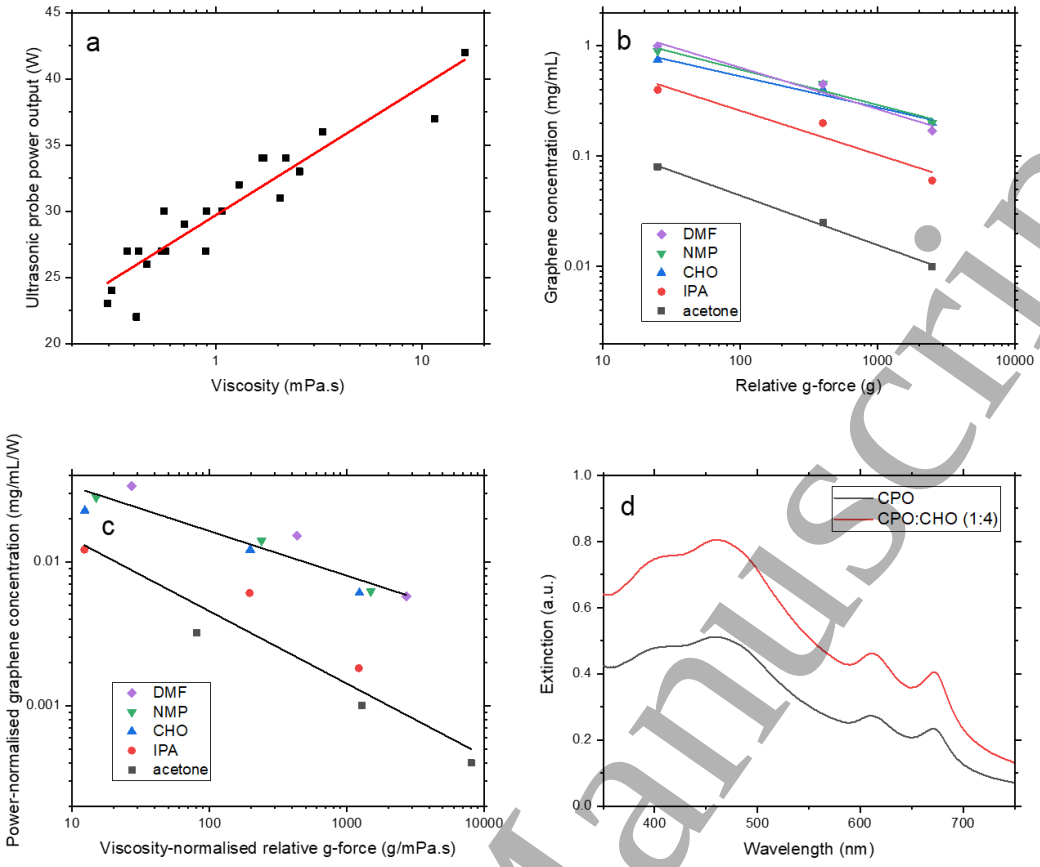

Figure 1: (a) Dependence of ultrasonic probe power output on solvent viscosity, showing a logarithmic relationship. (b) Graphene concentration in a range of 'good' and 'bad' solvents as a function of the relative g-force applied during centrifugation-based size selection, adapted from [14]. (c) Graphene concentration from (b) normalised to ultrasonic power output, as a function of viscosity-normalised relative g-force, to account for the influence of viscosity on both exfoliation and size selection. (d) UV-visible extinction spectra for MoS_2/CPO dispersion diluted into CPO and CHO before further centrifugation to illustrate the influence of viscosity.

Figure 1(a) shows the ultrasonic power output, measured by the instrument as the power required to drive the fixed-amplitude oscillation of the probe, for a range of organic solvents (see Supplementary Information) as a function of their viscosity. The power output shows a clear logarithmic dependence, which results in low viscosity solvents such as acetone being subjected to only 60% of the power of

high-viscosity solvents such as cyclohexanone (CHO). Notably, many of the good solvents identified for liquid phase exfoliation have viscosity >1 mPas [1,12]. While high viscosity is typically correlated with high surface tension and Hansen parameters through the cohesive energy density, it is possible that previous analyses, which have neglected the effect of viscosity, may have overestimated the relative performance of more viscous solvents.

In addition to its influence on the ultrasonic power output, the viscosity of the liquid will influence centrifugation-based size selection, since viscous drag forces oppose the sedimentation of dispersed particles. Nanosheets in higher viscosity liquids will experience greater viscous drag than nanosheets of the same size and mass in a lower viscosity liquid. As such, they sediment more slowly leaving a higher concentration of larger and thicker nanosheets dispersed in the supernatant than for lower viscosity liquids. This leads to higher post-centrifugation mass concentrations in these higher viscosity liquids when centrifuged under the same conditions as lower viscosity dispersions, due to the inclusion of these larger nanosheets.

In order to illustrate the significance of the twofold contribution of viscosity to exfoliation and size selection yield, analysis has been performed using data from O'Neill et al.[14] on the concentrations of graphene in both 'good' and 'bad' solvents with both low and high viscosity where single centrifugation steps at different speeds have been used to size select the nanosheets in the supernatant. To show the influence of viscosity, we initially focus on acetone and isopropanol (IPA) as two so-called poorer solvents. Although both solvents have a large mismatch in relative surface tension and Hansen parameters compared to graphene, IPA has a six-times-greater viscosity η than acetone, ($\eta_{acetone}$ = 0.31 mPa.s, η_{IPA} = 2.04 mPa.s [15]). For comparison, cyclohexanone, *N*-methyl-2-pyrrolidone (NMP) and dimethylformamide (DMF) have been included as three so-called good solvents which are similarly well matched to graphene in surface tension and Hansen parameters but also with a range of different viscosities (η_{CHO} = 2.02 mPa.s, η_{NMP} = 1.67 mPa.s, η_{DMF} = 0.92 mPa.s [15]).

Figure 1(b) shows the concentration of graphene in the different solvents as a function of the relative *g*-force used for the centrifugation-based size selection. The differences in concentration between the good solvents and the poorer solvents can be attributed to the yield of few-layer nanosheets during the ultrasonic exfoliation process which is determined by the surface tension and Hansen parameter matching [14], although NMP is also known to be susceptible to sonochemical degradation which may influence exfoliation[16,17]. As the relative *g*-force is increased, larger and thicker nanosheets are preferentially sedimented, leaving smaller and thinner populations of nanosheets dispersed, as shown by the decreasing concentration, which is well described by a series of near-parallel power laws for all solvents.

Interestingly, at low relative *g*-force centrifugation, DMF has the highest relative graphene concentration, despite its lower viscosity, while the highest viscosity solvent, CHO, has the lowest concentration with NMP being intermediate. This suggests that initially, the detailed performance of good solvents is dictated by the chemical physics of surface tension and Hansen parameters more so than the fluid physics of viscosity. Conversely, as the centrifugation process proceeds to higher relative g-force the already-thinner population of nanosheets in DMF is subjected to further sedimentation which decreases the concentration below both CHO and NMP, where higher viscosity results in retention of larger and thicker nanosheets and therefore higher concentration.

Clearly, we require a viscosity-based normalisation of the centrifugation parameters in order to quantitatively compare solvents and more importantly to allow consistent size selection of few-layer nanosheets with controlled size and thickness. As concentration increases approximately linearly with the energy-per-unit-volume applied during exfoliation[18], the concentration dependence on relative g-force from Figure 1(b) can be normalised to the ultrasonic power delivered as described in Figure 1(a). The sedimentation rate of a given size will be proportional to the relative g-force R (contributing to the weight) and inversely proportional to η contributing to the viscous drag. This additional normalisation (Figure 1(c)) accounts for the variation in viscous drag experienced by nanosheets of the same size and mass under the same centrifugation conditions in solvents of different viscosity. As such, R/η allows for comparison of equivalent centrifugation conditions.

With this normalisation, CHO, NMP and DMF (and other 'good' solvents) can be compared when subjected to equivalent centrifugation, which indicates that DMF shows higher concentration relative to its viscosity-normalised centrifugation conditions than NMP and CHO. This suggests that for this exfoliation and size selection process, DMF is genuinely the best solvent in terms of concentration of the graphene relative to the centrifugation conditions, i.e. the DMF dispersion contains nanosheets which are smaller *and* at higher concentration than in NMP and CHO.

For the poorer solvents, acetone and IPA, the viscosity normalisation results in an even more significant shift where the 2500 *g* centrifugation in IPA is shown to be nearly equivalent to the 400 *g* centrifugation in acetone (roughly equal to the ratio of their viscosities). Under these viscosity normalised centrifugation conditions, the concentrations of graphene in acetone and IPA are comparable and the data could be considered to converge on a single power law for poorer solvents, where the surface tension and Hansen parameter mismatch makes these viscosity effects markedly more pronounced. Indeed, it is even possible that if physical properties of the solvent could be suitably accounted for (by controlling power delivered, correcting centrifugation for viscosity, etc.), acetone and IPA could be equally good (or bad) solvents for the exfoliation of few-layer graphene and other 2D materials.

To further illustrate the effect of viscosity on sedimentation, molybdenum disulfide (MoS_2) was exfoliated in cyclopentanone (CPO) by probe ultrasonication, with a centrifugation step applied to remove unexfoliated material. CPO has surface tension and Hansen parameters almost equivalent to the six-membered-ring analogue CHO[19], but has significantly lower viscosity (η_{CPO} = 1.23 mPa.s, η_{CHO} = 2.02 mPa.s[15]). To isolate the influence of this viscosity difference for these otherwise very similar solvents, the MoS_2/CPO dispersion was diluted by a factor of 5 into both CPO and CHO and subjected to further centrifugation. The similarities between CPO and CHO make it possible to have an identical population of nanosheets in solvents of different viscosities without requiring changes to the exfoliation and size selection procedures.

Figure 1(d) shows the UV-visible extinction spectra of the CPO- and CHO-diluted dispersions after the second centrifugation step. The concentration of the CHO-diluted sample, measured from the minimum at ~350 nm is around 50% higher than for the CPO-diluted sample, highlighting the effect of the

increased viscosity in reducing sedimentation rate and leaving a greater mass of nanosheets dispersed than in the CPO sample. In addition, there is a slight redshift of the A-exciton for the CHO-diluted sample suggesting higher average layer number. Moreover, using the length metric calculation outlined by Backes et al.[20] the nanosheets are on average 5% larger. It is evident that the lower sedimentation rate allows larger particles to remain suspended in the high-viscosity system, where they would be removed from a dispersion with lower viscosity. This highlights the importance of accounting for viscosity (at least in centrifugation-based size selection) to ensure the size, thickness and concentration of the 2D nanosheets being selected is consistent between different solvents.

With this empirical understanding of the influence of viscosity and concentration on centrifugation, it would be desirable to develop a quantitative model for size selection of few-layer 2D nanosheets of a given size or thickness in arbitrary solvents. This approach facilitates consistent selection irrespective of the efficiency of the exfoliation process itself. By extending the arguments about viscous drag and sedimentation rate, it is possible to develop a simple metric for the centrifugation parameters required to sediment nanosheets based on their physical properties and those of the solvent.

Firstly, we evaluate the force balance on nanosheets falling under their weight, buoyancy and viscous drag due to the liquid, as shown in Figure 2(a), to determine their terminal velocity and therefore sedimentation time for a given height of centrifuge tube. We estimate the effective drag radius of the nanosheets, as the geometric mean of the length, width and thickness, i.e. the cube root of the volume, which allows us to deduce a relationship between the *g*-time product (relative g-force R and time T in minutes) and the volume $V = \langle L \rangle \langle W \rangle \langle N \rangle$;

$$RT = \frac{\pi \eta h}{10(\rho_{2D} - \rho_l)\alpha V^{2/3}}, \quad (1)$$

where η is the viscosity of the liquid, h is the filling height of dispersion in the centrifuge tube, ρ_{2D} and ρ_l are the densities of the 2D material and the liquid respectively and α is a constant accounting

for the absolute volumes of the nanosheets. A full derivation is presented in the Supplementary Information. Effectively, the model describes the centrifugal processing required to draw sheets of volume V from the top of a centrifuge tube to the bottom. Interestingly, it suggests that there is a direct equivalence between relative centrifugal force and time. For instance, we see that 1 minute at 15000 g will result in equivalent sedimentation as 1 hour at 250 g or even 15000 minutes under gravity, provided the effects of diffusion-driven reaggregation are negligible.

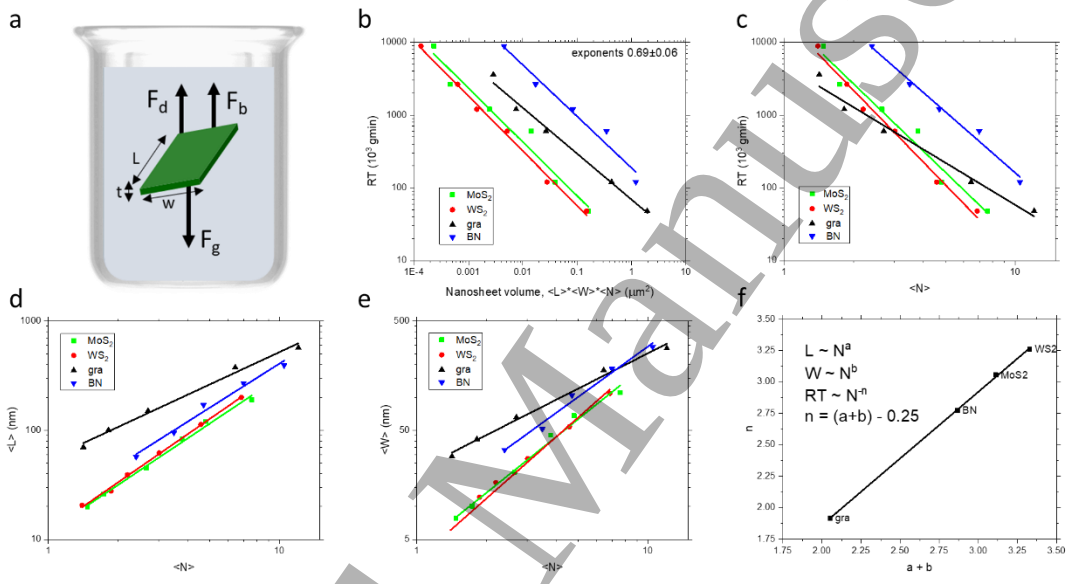

Figure 2: (a) Schematic showing force balance on a nanosheet falling under centrifuge-induced g-force, buoyancy and viscous drag. (b) Centrifugation g-time product as a function of nanosheet volume, measured from AFM, for size-selected dispersions of MoS_2, WS_2, graphene and BN, with power law fitting and exponents of 0.69±0.06. (c) Centrifugation g-time product as a function of average layer number for size-selected dispersions with power law fitting showing variation due to aspect ratio effects. (d) Length and (e) width of size-selected dispersions as a function of average layer to account for variability in g-time-$\langle N \rangle$ scaling in (c). (f) Scaling exponent for g-time against the sum of scaling exponents for length and width for different materials, indicating variability in (c) is fully accounted for by aspect ratio relationships.

In order to test this model, dispersions of MoS_2, tungsten disulfide (WS_2), graphene and boron nitride (BN) were prepared in aqueous sodium cholate solution by ultrasonic exfoliation and liquid cascade centrifugation[21]. In this process, the samples are produced by sedimentation and redispersion of the desired nanosheets which results in narrower size distributions compared with a single centrifugation step. The process is repeated under increasing centrifugation conditions to yield a series of samples with nanosheets of decreasing size and thickness. Specifically, in each step, the centrifugal acceleration was increased, but the time held at 2 hours. Identical vial geometries were used across the four data sets. The size-selected samples were characterised by statistical atomic force microscopy. The longest dimension (L), dimension perpendicular to this (width, W) and thickness were measured on 200-250 individual nanosheets. The apparent thickness was converted to layer number by the reported step height analysis of the material[18,20,22]. From such a statistical analysis, mean length $\langle L \rangle$, width $\langle W \rangle$ and layer number $\langle N \rangle$ for all samples was calculated and analysed as a function of their centrifugation g-time product.

These statistics can be used to calculate a mean nanosheet volume for each size-selected sample $V = \langle L \rangle \langle W \rangle \langle N \rangle$ which facilitates fitting of the data according to Equation 1. This data with the appropriate fitting is shown in Figure 2(b); in all cases, the g-time product also exhibits power law scaling with the volume with all exponents in the range 0.69 ± 0.06, indicating that the relationship $RT \sim V^{-2/3}$ well describes the size selection process.

While models similar to Equation (1) have been proposed[23] and verified[24] previously, little attention has been devoted to understanding the influence of aspect ratio on centrifugation. In practise, the volume of a nanosheet population is difficult to relate directly to the individual dimensions of interest; in particular the average layer number $\langle N \rangle$, which is most indicative of the degree of exfoliation. In contrast to the volume scaling, the power-law exponents for the g-time product variation with $\langle N \rangle$ vary significantly between different materials, as shown in Figure 2(c), presumably due to material-specific variance in the basal plane area. In order to better understand this variability between scaling laws, it would be desirable to account for the various aspect ratio relationships that contribute to the volume. The microscopic power law relationships between $\langle L \rangle$ and $\langle W \rangle$ and $\langle N \rangle$ are shown in Figure 2(d) and

(e) respectively. The pre-factors and exponents of these power laws relate to the length and width of the nanosheets at any given thickness with graphene and BN exhibiting larger pre-factors and smaller exponents than MoS_2 and WS_2, suggesting 'better' exfoliation to larger nanosheets at lower layer number.

These well-defined aspect ratio relationships facilitate parameterisation of nanosheet volume in terms of $\langle N \rangle$ with pre-factors and exponents which are characteristic of the exfoliation process, $\langle V \rangle \equiv \langle L \rangle \langle W \rangle \langle N \rangle \sim \langle N \rangle^a \langle N \rangle^b \langle N \rangle = \langle N \rangle^{a+b+1}$. Accordingly, by also parameterising the effective drag radius as $r \sim r_0 \langle N \rangle^c$ the centrifugation g-time product for size selection can be expressed in terms of the nanosheet thickness $\langle N \rangle$;

$$RT = \frac{\pi \eta h}{10(\rho_{2D} - \rho_l) k^2 \langle N \rangle^n} \quad (2)$$

where k is a 'shape factor' related to the aspect ratios of the nanosheets (see Supplementary Information for a description) and the exponent $n = a + b + 1 - c$.

This approach gives justification to the selection of centrifugation parameters to sediment a given size of nanosheets from a dispersion and potentially allows for the standardisation of size selection to ensure few-layer dispersions.

Figure 2(f) shows that the relationship between RT and $\langle N \rangle$ is well described by these underlying aspect ratio relationships. The exponent n increases linearly with the sum of the length and width exponents. In addition, the intercept (-0.25) indicates that the drag radius exponent $c = 1.25$ takes an empirical universal value for all of these materials. Given the drag radius has previously been shown to scale with volume with an exponent of 1/3, these relations can be equated to indicate that, on average, volume can be parameterised in terms of average layer number without the need to directly evaluate the aspect ratio of the nanosheets, such that $V \sim N^{15/4}$. This can be used to determine an average and idealised value for the exponent n of 2.5, since $RT \sim V^{2/3} \sim N^{5/2}$.

The idealised value of the exponent n quoted above, as an average of the data in Figure 2 for populations of well-exfoliated nanosheets, represents the ideal scaling for broad initial distributions of $\langle N \rangle$. In these samples there is sufficient content of few-layer nanosheets to allow progressively lower average layer number to be achieved through successive centrifugation steps, resulting in the expected scaling as observed in previous studies[21,22]. Deviations from this exponent can be attributed to variations in pre-centrifugation distribution such as in dispersions of large few-layer nanosheets wherein the average layer number will be reduced more gradually with centrifugation, since the nanosheet volume decreases more gradually with layer number. This results in reduced exponents ($n < 2.5$) and larger shape factors compared with the average case. By contrast, while dispersions with high-few layer content but smaller nanosheets can be considered well exfoliated, the nanosheet volumes scale more sharply with layer number and result in increased exponents ($n > 2.5$) and small shape factors. In addition, dispersions of comparatively poorly-exfoliated nanosheets with low few-layer content will retain higher average layer number after successive centrifugations, resulting in arbitrarily large exponents and unphysical shape factors, where the intuitive aspect ratio scalings above do not apply. As such, this approach can be used not only for size selection from dispersion but also for characterisation of the exfoliation process and degree of exfoliation achieved.

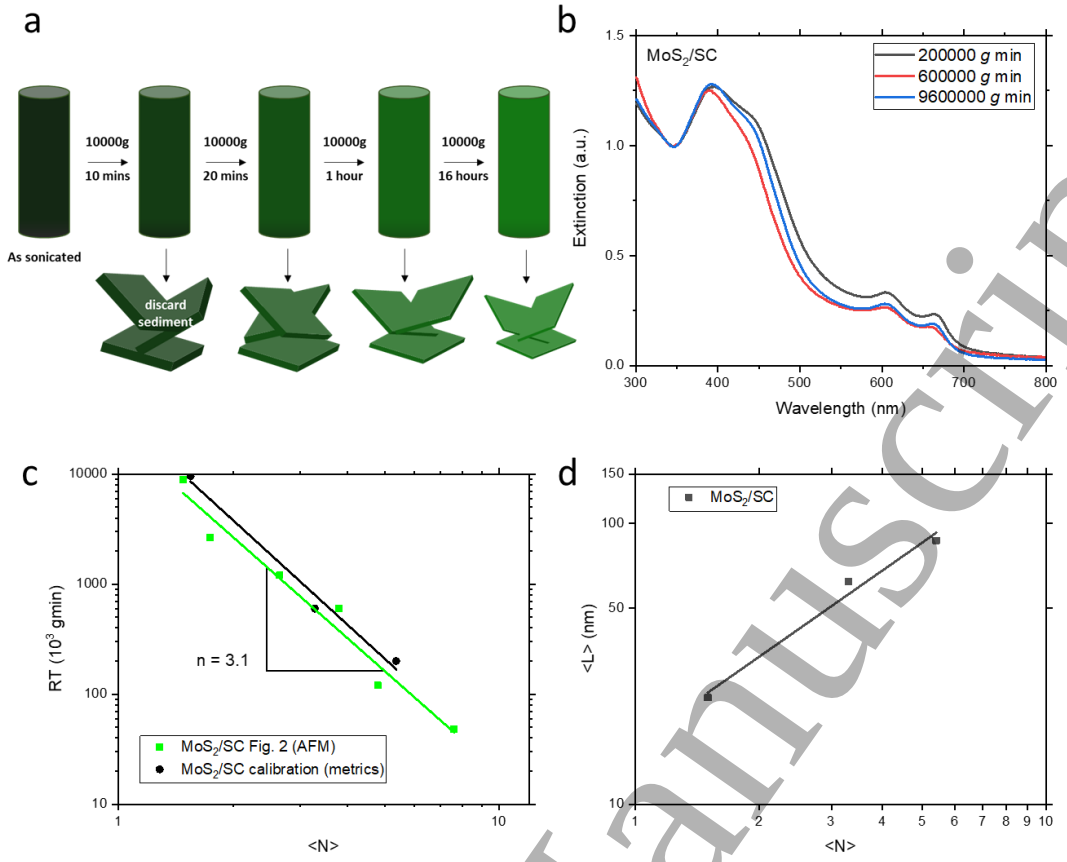

Figure 3: (a) Schematic of liquid cascade centrifugation process used for calibration experiment, including washing step used for transition metal dichalcogenides only. (b) UV-visible extinction spectra for dispersions of MoS_2 prepared in sodium cholate (SC) solution, as for the data in Figure 2, showing systematic blueshift with increasing centrifugation time used to determine layer number from spectroscopic metrics. (c) g-time as a function of $\langle N \rangle$ for size-selected MoS_2/SC dispersions shown alongside data measured by AFM from Figure 2(c), indicating excellent reproducibility of nanosheet populations under comparable processing conditions. (d) $\langle L \rangle$ versus $\langle N \rangle$ for measured from spectroscopic metrics for MoS_2/SC.

A calibration experiment can be performed to determine the shape factor and exponent for any given material and processing parameters. This involves exfoliation of the bulk material followed by liquid cascade centrifugation of the exfoliated nanosheets. The average layer number of each sample would be characterised, either by statistical atomic force microscopy (AFM) or using spectroscopic

metrics[20,22,25], and this would be used to fit against the g-time product to determine the exponent n and shape factor k for that material and process. Given this calibration, Equation (2) can be applied to determine centrifugation parameters to select nanosheets of any given thickness in future experiments. Figure 3(a) shows a centrifugation cascade with the RT values selected to give the greatest possible applicability for a range of solvent viscosities, material densities, shape factors and exponents, where the average layer numbers sedimented can be characterised by spectroscopic metrics in order to perform a calibration experiment.

The UV-visible extinction spectra for dispersions of MoS_2 exfoliated in sodium cholate solution (as for the data in Figure 2) and size selected by liquid cascade centrifugation are shown in Figure 3(b). These exhibit a clear blueshift of the A-exciton with increasing RT, associated with decreasing average layer number. The $\langle N \rangle$ values are determined from the respective spectroscopic metrics[20–22,25] and fitted to determine the shape factor and exponent, shown in Figure 3(b). Note that in this experiment, the centrifugation speed was kept constant, while the time was varied in order to expedite the low g-time centrifugation steps. While a combination of varying relative g-force and time can be used to preferentially select higher or lower aspect ratio nanosheets, we find that using one approach or the other gives broadly similar results. Furthermore, these calibration experiments were performed with a smaller volume ultrasonic probe, smaller volumes and correspondingly shorter sonication time than for the experiments in Figure 2 (VCX130, 30 mL and 3 hours cf. VCX750, 80 mL and 5 hours). Nevertheless, when using the same surfactant and similar initial concentrations of MoS_2 and surfactant, we find excellent agreement in the centrifugation-size dependence indicating the robustness of the g-time equivalence and the reproducibility of nanosheet populations under comparable processing with both exponents around 3.1.

After performing this calibration experiment, it is possible to use the fit parameters (shape factor and exponent) to determine the g-time product required to prepare dispersions of nanosheets with predetermined properties. For MoS_2, for example, it may be desirable to have dispersions of nanosheets with N-independent band gap ($N > 6$) to prevent few-layer nanosheets acting as charge traps in devices while maintaining the aspect ratio as much as possible to produce highly-aligned networks (perhaps

$N < 10$). Using this model, the centrifugation conditions required to sediment nanosheets with $N > 10$ in the first step and $N > 6$ in a subsequent step can calculated and implemented to produce dispersions with layer number in the desired range.

This methodology facilitates rapid and representative characterisation of a range of liquid exfoliated layered nanomaterials. The use of a simple physically-grounded model describing the size selection process facilitates calibration of the size selection procedure and optimisation of the exfoliation process. We believe that this approach will allow other researchers in the field to improve the selectivity and efficiency of their processes, whilst also providing a framework for standardised comparison of results.

Conclusion

We have developed a size selection model for liquid-exfoliated 2D nanosheets, which facilitates standardisation of centrifugal processing for production of dispersions with controlled size and thickness. We demonstrate that the influence of viscosity on ultrasonic exfoliation may have been neglected in previous analyses and that, when viscosity is suitably accounted for, the results are well described by the chemical physics (surface tension and Hansen parameter matching) for both 'good' and 'bad' solvents. By using a simple force balance model, it is possible to determine centrifugation parameters for different materials and solvents. This model can be calibrated for a given exfoliation process to facilitate controlled size selection of nanosheets or to characterise and compare exfoliation processes.

References

1. Coleman, J. N. *et al.* Two-Dimensional Nanosheets Produced by Liquid Exfoliation of Layered Materials. *Science* **331**, 568–571 (2011).

2. Lin, Z., Mcnamara, A., Liu, Y., Moon, K. & Wong, C.-P. Exfoliated hexagonal boron nitride-based polymer nanocomposite with enhanced thermal conductivity for electronic encapsulation. *Compos. Sci. Technol.* **90**, 123–128 (2014).

3. Bang, G. S. *et al.* Effective Liquid-Phase Exfoliation and Sodium Ion Battery Application of MoS2 Nanosheets. *ACS Appl. Mater. Interfaces* **6**, 7084–7089 (2014).

4. Higgins, T. M. *et al.* Electrolyte-Gated n-Type Transistors Produced from Aqueous Inks of WS2 Nanosheets. *Adv. Funct. Mater.* **0**, 1804387

5. Kang, J. *et al.* Solvent Exfoliation of Electronic-Grade, Two-Dimensional Black Phosphorus. *ACS Nano* **9**, 3596–3604 (2015).

6. Song, F. & Hu, X. Exfoliation of layered double hydroxides for enhanced oxygen evolution catalysis. *Nat. Commun.* **5**, 4477 (2014).

7. Lotya, M., King, P. J., Khan, U., De, S. & Coleman, J. N. High-Concentration, Surfactant-Stabilized Graphene Dispersions. *ACS Nano* **4**, 3155–3162 (2010).

8. Khan, U., O'Neill, A., Lotya, M., De, S. & Coleman, J. N. High-Concentration Solvent Exfoliation of Graphene. *Small* **6**, 864–871 (2010).

9. Finn, D. J. *et al.* Inkjet deposition of liquid-exfoliated graphene and MoS2 nanosheets for printed device applications. *J. Mater. Chem. C* **2**, 925–932 (2014).

10. Large, M. J. *et al.* Functional liquid structures by emulsification of graphene and other two-dimensional nanomaterials. *Nanoscale* (2018). doi:10.1039/C7NR05568D

11. Hernandez, Y., Lotya, M., Rickard, D., Bergin, S. D. & Coleman, J. N. Measurement of Multicomponent Solubility Parameters for Graphene Facilitates Solvent Discovery. *Langmuir* **26**, 3208–3213 (2010).

12. Hernandez, Y. *et al.* High-yield production of graphene by liquid-phase exfoliation of graphite. *Nat. Nanotechnol.* **3**, 563–568 (2008).

13. Sesis, A. *et al.* Influence of acoustic cavitation on the controlled ultrasonic dispersion of carbon nanotubes. *J. Phys. Chem. B* **117**, 15141–15150 (2013).

14. O'Neill, A., Khan, U., Nirmalraj, P. N., Boland, J. & Coleman, J. N. Graphene Dispersion and Exfoliation in Low Boiling Point Solvents. *J. Phys. Chem. C* **115**, 5422–5428 (2011).

15. Lide, D. R. *CRC Handbook of Chemistry and Physics, 85th Edition*. (CRC Press, 2004).

16. Ogilvie, S. P. *et al.* Considerations for spectroscopy of liquid-exfoliated 2D materials: emerging photoluminescence of N -methyl-2-pyrrolidone. *Sci. Rep.* **7**, 16706 (2017).

17. Jawaid, A. *et al.* Mechanism for Liquid Phase Exfoliation of MoS2. *Chem. Mater.* **28**, 337–348 (2016).

18. Paton, K. R. *et al.* Scalable production of large quantities of defect-free few-layer graphene by shear exfoliation in liquids. *Nat. Mater.* **13**, 624–630 (2014).

19. Hansen, C. M. *Hansen Solubility Parameters: A User's Handbook, Second Edition*. (CRC Press, 2007).

20. Backes, C. *et al.* Edge and confinement effects allow in situ measurement of size and thickness of liquid-exfoliated nanosheets. *Nat. Commun.* **5**, 4576 (2014).

21. Backes, C. *et al.* Production of Highly Monolayer Enriched Dispersions of Liquid-Exfoliated Nanosheets by Liquid Cascade Centrifugation. *ACS Nano* **10**, 1589–1601 (2016).

22. Griffin, A. *et al.* Spectroscopic size and thickness metrics for liquid-exfoliated h-BN. *Chem. Mater.* (2018). doi:10.1021/acs.chemmater.7b05188

23. Nacken, T. J., Damm, C., Walter, J., Rüger, A. & Peukert, W. Delamination of graphite in a high pressure homogenizer. *RSC Adv.* **5**, 57328–57338 (2015).

24. Biccai, S. *et al.* Exfoliation of 2D materials by high shear mixing. *2D Mater.* (2018). doi:10.1088/2053-1583/aae7e3

25. Backes, C. *et al.* Spectroscopic metrics allow in-situ measurement of mean size and thickness of liquid-exfoliated graphene nanosheets. *Nanoscale* **8**, 4311–4323 (2016).